Ali S. Jalal
Department of Information and Communication, Engineering, College of Information Engineering, Al-Nahrain University, Baghdad, Iraq.
ali.sadeq@coie-nahrain.edu.iq

Marwa H. Jwair
Department of Information and Communication Engineering, College of Information Engineering, Al-Nahrain University, Baghdad, Iraq.

Received on: 14/08/2017
Accepted on: 23/11/2017

On the Performance of a Microstrip Antenna Based UC-PBG Structures for UHF RFID Readers

Abstract- *Microstrip antennas suffer from low gain bandwidth product due to surface wave effects and aperture diffractions that limit their use for long-range communications. On top of that, the difficulty of achieving a pure circularly polarized radiation with high gain due to the feeding structure effects. This paper is subjected to design a gain enhanced circularly polarized patch antenna using Uniplanar Compact-Photonic Band Gap (UC-PBG) structu.res for UHF RFID applications. The patch is structured as truncated corners with cross slots at the centre mounted on an FR-4 epoxy substrate of 1.6mm thickness with an overall area of 188×188mm^2. The UC-PBG is constructed of two layers; each is made of 7×7 unit cells, separated by 20mm mounted from the top of the patch at 30mm height. The unit cell characterizations are evaluated in terms of their S-parameters and dispersion diagram CST-MWS environment. The antenna shows a boresight gain of about 8.2 dBi at 915MHz with a front to back ratio (F/B) of 13dB. The benchmark enhancement in boresight gain after adding the UC-PBG layers is found to be 3.4 dBi with a radiation efficiency of 87%. Finally, an excellent agreement is achieved between the obtained measurements and numerical results.*

Keywords- *Circular polarization, RFID, UHF, UC-PBG.*

How to cite this article: A.S. Jalal and M.H. Jwair, "On the Performance of a Microstrip Antenna based UC-PBG structures for UHF RFID Readers," *Engineering and Technology Journal*, Vol. 36, Part A, No. 5, pp. 480-487, 2018.

1. Introduction

Last decades, RFID technology advanced remarkably in different fields including modern technology for auto-identification systems and storing data by tags and transponders [1]. The RFID concept was initiated during the Second World War [2]. RFID systems usually consist of three main parts: Readers, tags, and host [3]. The operation scenario of RFID systems is based on sending a signal from the reader to the tag. Then, the tag identifies the signal and stores the information. Finally, the host realizes the decoded data from readers [4]. In 1948, Stockman articled the first RFID system [2]. Later, the RFID systems were developed rapidly in different frequency bands including Low Frequency (LF) at 125-134.2 kHz, High Frequency (HF) (13.56 MHz), Ultra-High Frequency (UHF); (433 MHz, 860-960 MHz) and Microwave Frequency (MWF) (2.45 GHz, 5.8 GHz) [3]. In general, RFID systems are classified into passive and active systems, besides to a semi-active system, which has a combination of active and passive characteristics [5]. The passive RFID systems are based on a Tag that does not have an internal power source where it is fully managed by the reader [6]. This type suits smart labels, supply chain management, file tracking, race timing, and access control applications. For active RFID systems, tags are powered by batteries to transmit the data continuously that are usually used for real-time tracking assistant. Usually, active tags can provide a longer communication range than passive tags but are much more expensive [5]. Last decades, the applications of the UC-PBG structures, in the microwave devices [7] started to dominate over other passive structures. Generally, these structures were designed as a periodical crystal patterns and slots are etched in the ground planes [8]. Although, these configurations were already used for microstrip antenna designs, antennas experienced from strong backward radiation that reduces the bore-sight gain [9]. Therefore, many researchers were attracted to enhance antenna performance by applying UC-PBG structures. Among many others, Electromagnetic Band Gap (EBG) and/or UC-PBG were introduced in [7-11], to utilize an improvement in the antenna gain for their versatility and ease of fabrication. In this context, various geometries have found their way in designing circularly polarized antennas for RFID readers' applications [12-22]. Therefore, it is the subject for this research to construct a circularly polarized microstrip antenna with a high gain mounted underneath of a double layered UC-PBG

https://doi.org/10.30684/etj.36.5A.1
2412-0758/University of Technology-Iraq, Baghdad, Iraq

structure with 7×7 unit cell arrays. Then, the proposed UC-PBG structure is designed based on finite uniform 2D periodical metal structures to enhance the antenna gain. It is found that the combination of the UC-PBG structure with the microstrip antenna is appropriate for many applications in the UHF frequency band including the RFID readers. The antenna performance including the S_{11} spectra and radiation patterns; before and after adding the UC-PBG layers are tested and simulated using FIT based on CSTMWS formulations. The UC-PBG CP antenna is fabricated and measured. Finally, obtained results are also validated using FEM-based HFSS software package.

2. Antenna and UC-PBG Geometrical Design

The proposed antenna geometry is constructed of a microstrip circularly polarized patch printed on a Flame Retardant (FR-4) epoxy substrate, ε_r = 4.3, and $tan\delta$ = 0.02, with thickness (h) of 1.6 mm. To achieve a circularly polarized microstrip patch, a truncated rectangular patch with crossed line slots at its center is chosen for ease of fabrication. An SMA coaxial connector of 50 Ω characteristics impedance is used to feed the patch structure. The feeding point is located at the patch length center with an offset from the width center of 4 mm. Figure 1 and Table 1 show all related geometrical details of the patch, substrate, and the feed location.

Table 1: Dimensions of the patch

Parameter	L	W	L_p	W_P	GAP	S
Dimension (mm)	188	188	106	74	5	18.5

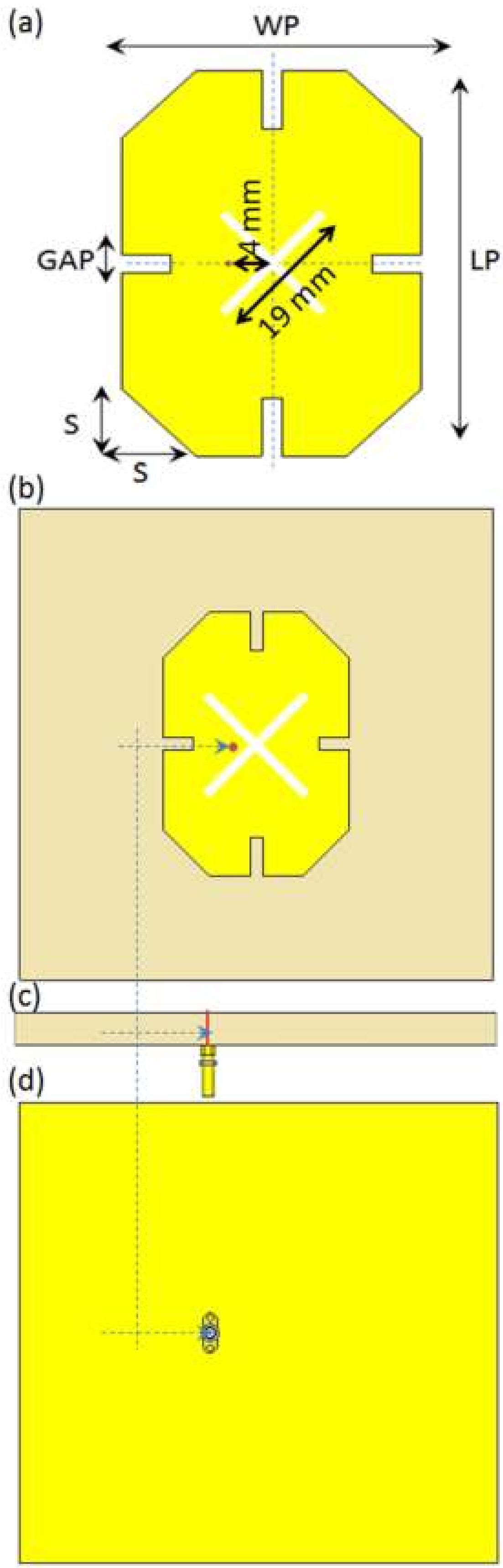

Figure 1: Antenna geometry: (a) Patch structure, (b) Front view, (c) Side view, (d) Back view.

The UC-PBG structure is constructed of two layers with 7×7 unit cells array. Two concentric rings are shaped as a continuous closed square trace and a split circle with a certain gap to function as resonance window. The capacitive coupling - that may occur between the UC-PBG layers - improves their resonance around a certain frequency band. The square ring dimensions are 26 × 26 mm^2, while, the circular ring radius is 10 mm. Each trace width is fixed to 1 mm, while, the air gap between the two rings is 2 mm. Each two adjacent unit cells are separated by 1 mm air gap. To achieve the maximum gain, the first UC-PBG layer is placed at 30 mm from the top of the patch and the second layer is located at 20 mm from the top of it. The proposed UC-PBG layers are holed on foam bases as depicted in Figure 2.
Now, the antenna structure is combined with the UC-PBG layers as presented in Figure 3. According to the standard optical rules, the reflective index, the incident angle, the source position, the focal length of the lens, and the HPBW might be determined from the ray tracing analysis [23].

3. Numerical Simulation and Results

I. UC-PBG Characterizations

In this section, the parametric study is invoked to evaluate the proposed UC-PBG layers. The numerical simulation is conducted with the CST-MWS to the proposed unit cell inside a fictitious waveguide center as to mimic quasi-TEM modes [24]. From the evaluated S_{11} and S_{21} in terms of magnitude and phase, it is found that there is no specific resonance within the frequency band from 0.8 GHz up to 1 GHz as seen in Figure 4. A parametric study is investigated on the strip width, gap, and inner radius to monitor the effects of losses at 915 MHz as listed in Table 2.

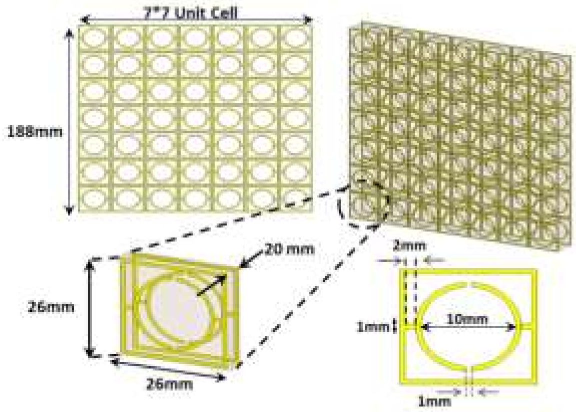

Figure 2: UC-PBG Geometry.

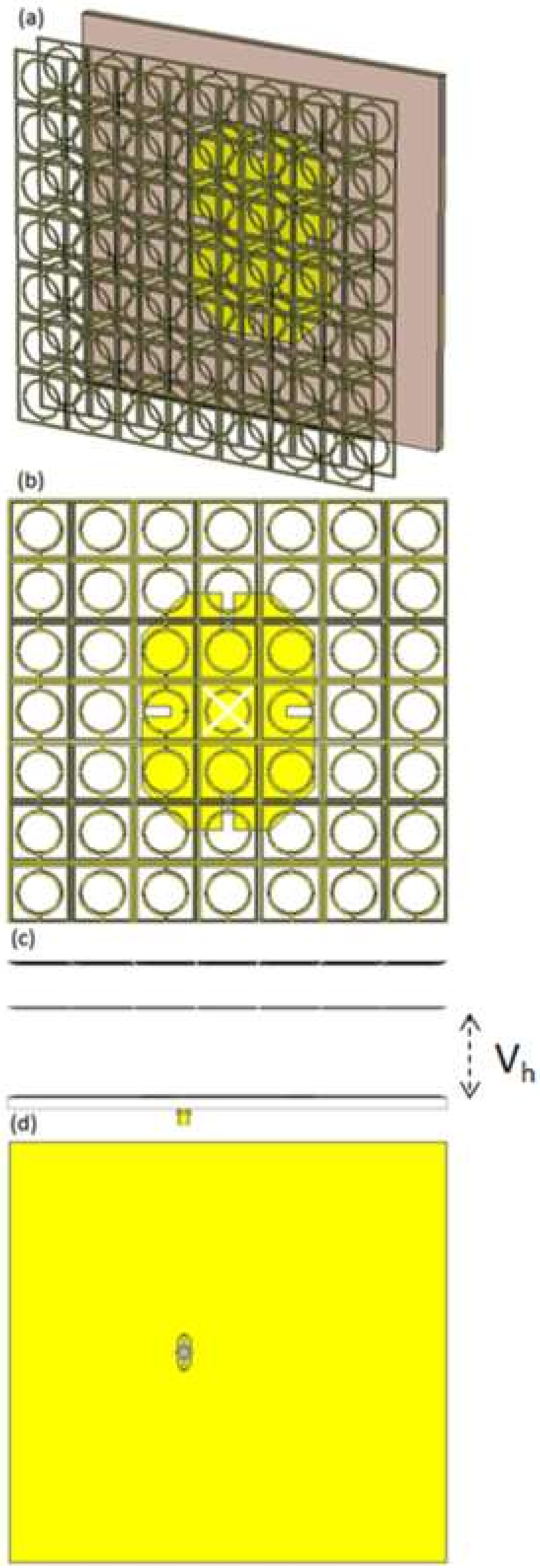

Figure 3: Microstrip antenna based on UC-PBG Layers: (a) 3-D view. (b) The structure front view (c) side view (d) back view.

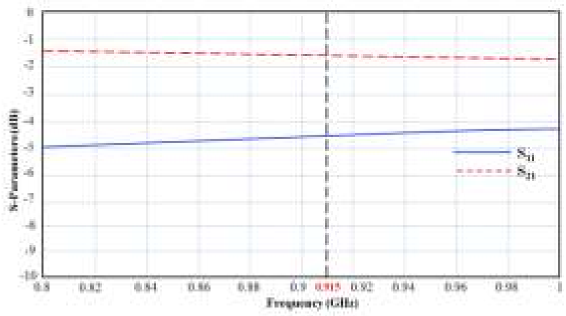

Figure 4: S-parameters spectra of the proposed unit cell based (double face).

Table 2: The evaluated losses with respect to changing the double face unit cell dimensions at 915 MHz.

Parameter	Change (mm)	S_{11} (dB)	S_{21} (dB)	Losses (%)
Strip-width	2	-4.79	-1.75	2.71
	3	-4.74	-1.82	9.3
	4	-4.75	-1.79	7.03
Gap	1	-4.76	-1.76	3.48
	1.5	-4.77	-1.75	4.86
	2	-4.79	-1.75	2.71
Inner-Radius	5	-4.74	-1.77	4.11
	7	-4.74	-1.77	2.31
	9	-4.76	-1.76	3.48

Next, the separation distance effects between the UC-PBG layers are studied regarding S-parameters as seen in Figure 5. It is found that increasing the separation distance may lead to an increase in the conservation losses due to the capacitive effects. Therefore, it is fixed around 20 mm, while, when it goes below this limit it shows negative effects on the paraxial rays emerge. After that, a parametric study based on a full-wave numerical analysis as shown in Figure 6 is applied to study the required number of the unit cells in the UC-PBG layers starting from 1×1, 3×3, 5×5, and 7×7. It is observed that a significant reduction in the field diffraction takes place in the same amount of unit cell increment. Therefore, the unit cell number increase may increase the focusing effects; however, the size criterion limits the designer goals. Therefore, the authors are satisfied with the 7×7 array; where, after that, the effect of diffraction becomes almost negligible.

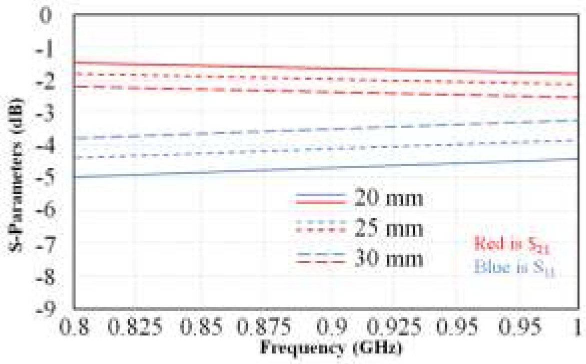

Figure 5: UC-PBG performance regarding S-parameters spectra of the proposed unit cell with different separations distance.

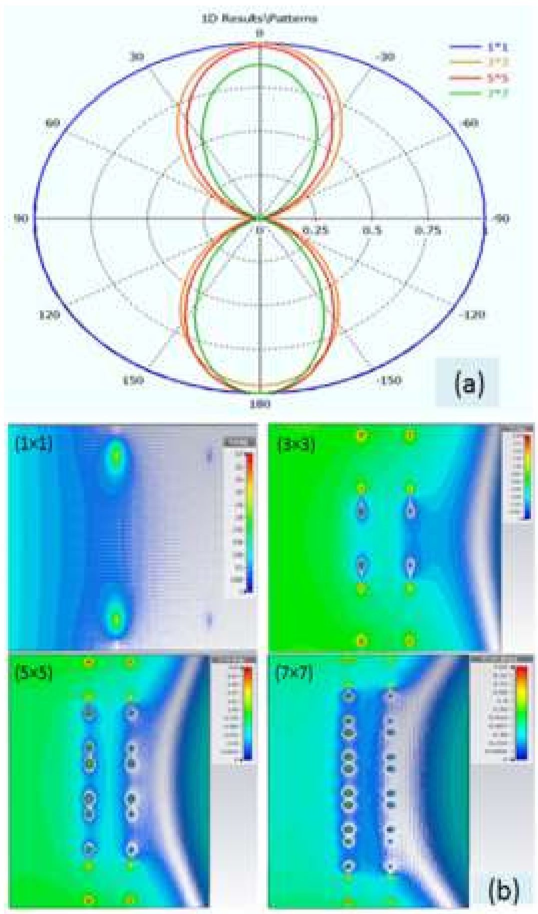

Figure 6: Plane wave results at 915 MHz; (a) 2-D view and (b) 3-D view.

For an additional characterization, the dispersion diagram using CST-MWS formulations is discussed in the First Brillouin Zone (FBZ) as seen in Figure 7. It is found that the unit cell shows no dispersion in the diagonal direction (χ-M), however, on the other sides, the unit cell is found to be very dispersive when the emerged tangential beams are impinging oppositely leading to field cancellation on the UC-PBG.

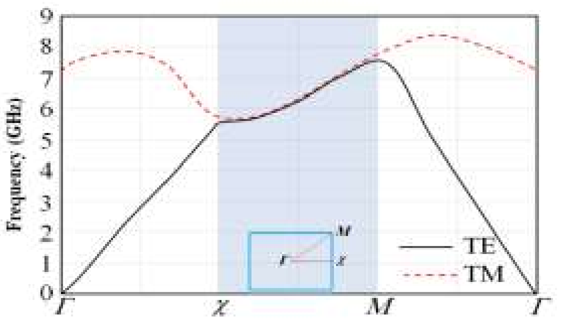

Figure 7: Dispersion diagram at the FBZ.

II. Antenna Performance

In this section, the antenna design based on the proposed UC-PBG structure is studied to provide the maximum matching at 915 MHz. In this study, the antenna performance is tested in terms of S_{11} spectra and radiation patterns as seen bellow:

1) A numerical study is performed without the UC-PBG layers, then, the patch dimensions and the feed location are optimized to be excellently matched at 915 MHz. It is found that the antenna shows excellent matching, $|S_{11}|$<-11 dB, with a bore sight gain of 4.8 dBi. Figure 8 shows the S_{11} spectrum and radiation patterns at the ϑ- and φ-plans. Nevertheless, the antenna shows a circular polarization as seen in Figure 8(b). This is achieved by using cross-slots at the center and truncated corners of the patch with rectangular slits along the length and the width.

2) The best UC-PBG location (V_h) from the antenna patch is studied by running a parametric study from 10 mm to 70 mm in steps of 10mm. As seen in Figure 9(a), the S_{11} spectrum changes due to the capacitive coupling effects on the patch structure. Moreover, it is found that the best UC-PBG location to provide the maximum bore sight gain is at 30 mm from the patch top as can be seen in Figure 9(b).

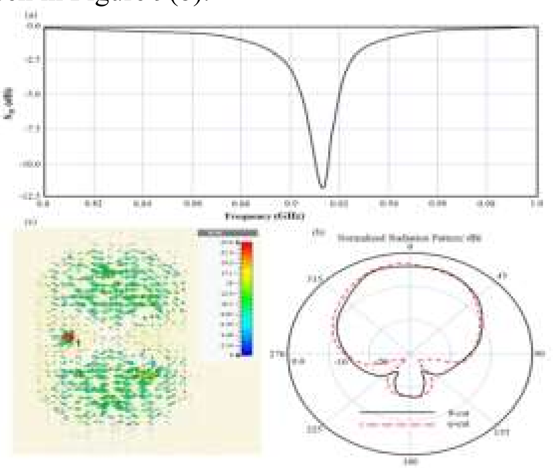

Figure 8: The performance of the proposed antenna without UC-PBG Layers: (a) S11, (b) Radiation Patterns, (c) Current Distribution.

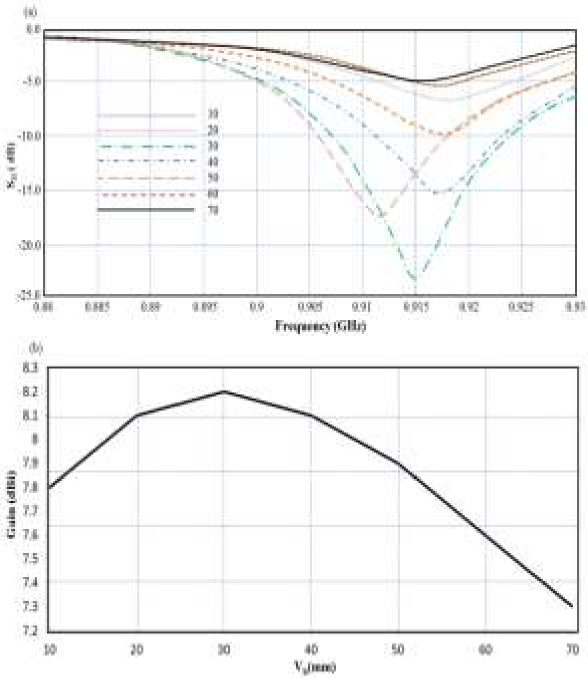

Figure 9: Parametric study of the proposed UC-PBG Layers from the antenna structure: (a) S_{11} and (b) bore sight gain.

4. The Optimal Antenna Performance and Validation

The obtained antenna results are re-evaluated numerically using FEM based on HFSS formulations and compared to the CST MWS results as seen Figure 10. It is found that the investigated study shows excellent agreements in terms of S_{11} and radiation patterns. The antenna shows a maximum gain of 8.2 dBi at 915 MHz with an axial ratio of 2.5 dB. Now, the proposed antenna is fabricated as seen in Figure 11. Then, the antenna is tested using a Vector star MS4642A Series Microwave Vector Network Analyzer (VNA) inside an anechoic chamber after running cables calibration using short, open, and 50 Ω loads. From measurements, it is found that the S_{11} spectrum shows a frequency resonance around 918 MHz with a bore sight gain around 8.2 dB as seen in Figure 12.

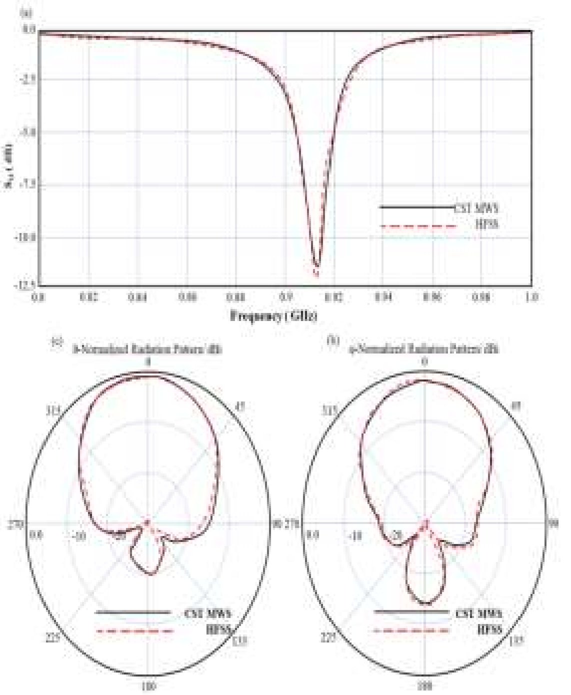

Figure 10: The proposed microstrip antenna based UC-PBG Layers: (a) S_{11}, (b, c) radiation patterns

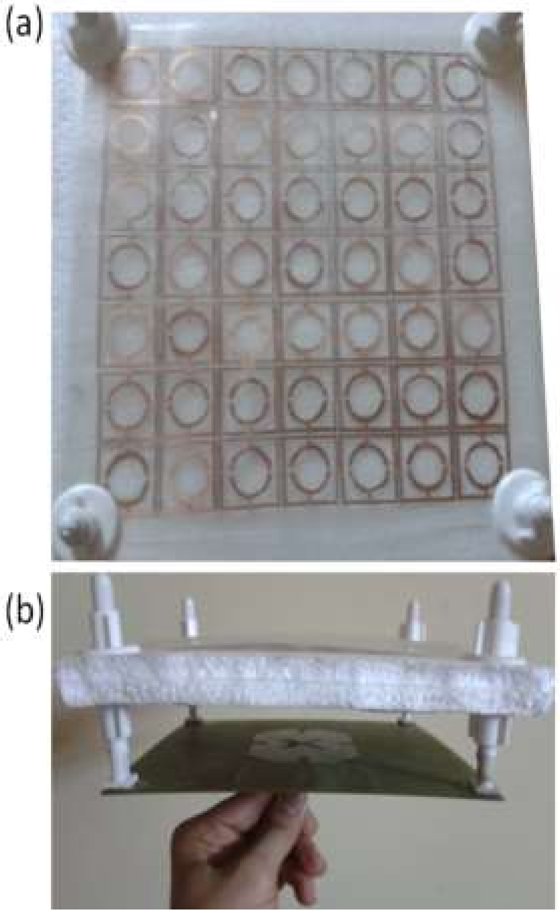

Figure 11: The fabricated prototype with the UC-PBG layers; (a) Top view (b) Side view.

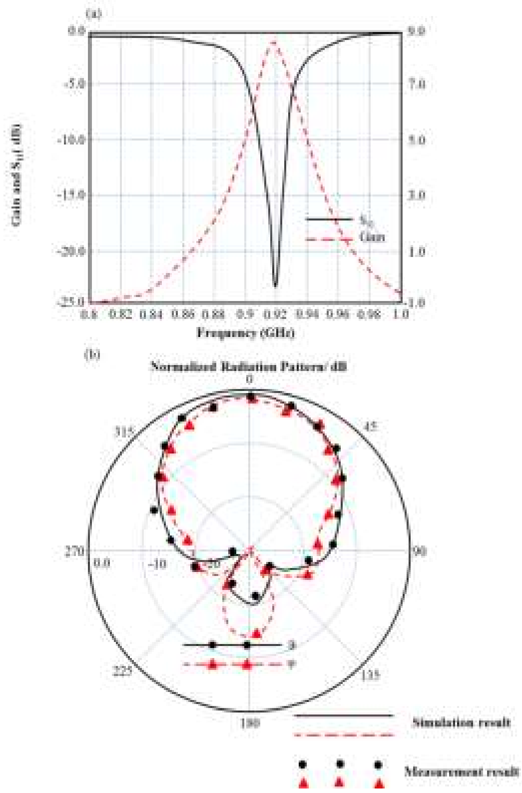

Figure 12: Microstrip antenna based UC-PBG Layers measurements: (a) Gain and S_{11} spectra and (b) radiation patterns for measured and simulated results.

Table 3 shows a survey comparison between the published contributions in terms of antenna size and gain at UHF band with the proposed work. It is found that the proposed antenna provides the highest gain with minimum dimensions in comparison to published previous results.

5. Conclusion

Tables In this paper, a circularly polarized patch antenna based on a UC-PBG structure for UHF RFID readers is designed, fabricated and measured. The UC-PBG characterizations in terms of S-parameters, reflection phase, and band gap properties in the FBZ are computed. It is found that the proposed UC-PBG layers provide positive propagation slope with no band gap region to suit the antenna gain enhancement at 915 MHz. The antenna performance after introducing the UC-PBG layers is tested to realize the effects of UC-PBG improvement to provide an enhanced bore sight gain of 8.2dBi and F/B ratio of 13dB, where, the antenna gain without the UC-PBG layers is found to be 4.8 dBi. Finally, the obtained results are validated numerically with CST MWS and HFSS software packages to match the antenna measurements excellently.

Table 3: Comparison with Related Publications

References Number	Frequency range (MHZ)	Max gain (dB)	3-db Beam Width (Degree)	Size (L×W×H) (mm^3)
Ref. [12]	864-873	4.0	NA	184×174×3.175
Ref. [13]	866	4	53	415×415×4.15
Ref. [14]	922	5	NA	100×100×1.6
Ref. [15]	920-925	3.7	82	120×120×1.6
Ref. [16]	915	6	NA	150×150×13
Ref. [17]	920	6.6	NA	220×220×32.6
Ref. [18]	925	3.8	81	110×110×6.6
Ref. [19]	920	3.9	80	105×105×50
Ref. [20]	901-930	7.3	75	150×150×34
Ref. [21]	915	8.9	NA	220×220×14
Ref. [22]	877-945	6.3	NA	174×171×10
Proposed work	915	8.2	64	188×188×50

References

[1] A.S.A. Jalal, Alyani Ismail, Adam R.H. Alhawari, Mohd F.A. Rasid, Nor K. Noordin, and Mohd A. Mahdi, “Miniaturized Metal Mount Minkowski Fractal RFID Tag Antenna with Complementary Split Ring Resonator,” Progress In Electromagnetics Research C, Vol. 39, 25-36, 2013.

[2] A.S.A. Jalal, Alyani Ismail, Adam R.H. Alhawari, Mohd F.A. Rasid, Nor K. Noordin, and Mohd A. Mahdi, “Metal Mount Fractal RFID Tag Antenna with Complementary Split Ring Resonator,” in Proceeding of the 2013 IEEE International Conference on RFID Technologies and Applications, 04–05 September 2013 Johor Bahru, Malaysia.

[3] A.R.H. Alhawari, Alyani Ismail, Ali S.A. Jalal, Raja S.A.R. Abdullah, Mohd F.A. Rasid, “U-Shaped Inductively Coupled Feed RFID Tag Antennas for Gain Enhancement,” Electromagnetics, Vol. 34, 487-496, 2014.

[4] N.H. Daud, A Ismail, ARH Alhawari, A Sali, MF Rasid, Ali S. A. Jalal, "Integration of split ring resonators (SRRs) to UHF RFID tag antenna for size reduction," in proceeding of the IEEE 4th International Conference on Engineering Technology and Technopreneuship (ICE2T), 2014.

[5] A.S.A. Jalal, “Passive RFID Tags,” Wulfenia Journal, Vol. 22, No. 12, pp. 415-435, DEC. 2015.

[6] M. Haleem Jwair, Ali Sadeq Abdulhadi Jalal, “A Gain Enhanced Circularly Polarized Microstrip Antenna for RFID Readers Applications,” International Journal of Scientific & Engineering Research, Volume 7, Issue 9, September-2016.

[7] F.R Yang, K.P Ma, Y. Qian and T. Hoh “Uniplanar compact photonic band gap (UC-PBG) structure and its applications for microwave circuits,” IEEE Trans Microwave Theory Tech, Vol. 47, pp 1509-1514, 1999.

[8] T.A. Elwi, A. Imad and Y. Alnaiemy, “A Miniaturized Lotus Shaped Microstrip Antenna Loaded with EBG Structures for High Gain-Bandwidth Product Applications,” Progress In Electromagnetics Research C, volume 60, pp. 157-167, December 2015,

[9] X. B. Sun, M.Y. Cao, J.J. Hao, and Y.J. Guo, “A rectangular slot antenna with improved bandwidth,” AEU - Int. J. Electron. Commun. Vol. 66, No. 6, pp. 465–466, 2012.

[10] O.A. Ibrahim, T.A. Elwi, N.E. Islam, “Gain Enhancement of Microstrip Antennas Using UC-PBG Layer,” Canadian Journal on Electrical and Electronics Engineering, volume 3, ID: EEE-1211-016, pp. 480-483, no. 9, November 2012.

[11] T.A. Elwi, H.M. Al-Rizzo, N. Bouaynaya, M.M. Hammood, and Y. Al-Naiemy, “Theory of gain enhancement of UC–PBG antenna structures without invoking Maxwell’s equations: an array signal processing approach,” Progress In Electromagnetics Research B, volume 34, pp. 15-30, August 2011.

[12] Xi Chen, Guang Fu, Shu-Xi Gong, Ya-Li Yan, and Wei Zhao, “Circularly Polarized Stacked Annular-Ring Microstrip Antenna with Integrated Feeding Network for UHF RFID Readers,” IEEE Aantennas and Wireless Propagation Letters, VOL. 9, 2010.

[13] C. Phongcharoenpanich and Sitthichai Dentri, “Circularly Polarized UHF-RFID Antenna using Defected Rectangular Plate on the Ground Plane,” IEEE Asia-Pacific Conference on Antennas and Propagation, August 27-29, 2012.

[14] Sylvain Pflaum, Philippe Le Thuc, Georges Kossiavas and Robert Staraj, “Circularly Polarized Patch Antenna using UC-PBG structure for RFID Readers,” IEEE, 2013.

[15] C. Phongcharoenpanich and Benjaporn Sricharoen, “Dual-Band Circularly Polarized Rectangular Loop Slot Antenna for UHF-RFID Reader,” IEEE, 2012.

[16] Heng-Tung Hsu, Ting-Jui Huang, “Aperture-Coupled Dual-band Circularly Polarized Antenna for RFID Reader Applications,” IEEE Cross Strait Quad-Regional Radio Science and Wireless Technology Conference, 2012.

[17] Youn-Kwon Jung and Bomson Lee, “Dual-Band Circularly Polarized Microstrip RFID Reader Antenna Using Metamaterial Branch-Line Coupler,” IEEE Antennas Propag Vol. 60, No. 2, FEB. 2012.

[18] Qiang Liu, Junyu Shen, Jungang Yin, Hongli Liu, and Yuanan Liu, “Compact 0.92/2.45-GHz Dual-Band Directional Circularly Polarized Microstrip Antenna for Handheld RFID Reader Applications,” IEEE Antennas Propag, Vol. 63, No. 9, SEP. 2015.

[19] Fong Chen, Chia-Mei Peng, and Guan-Lin Chen, “A novel reduced size microstrip antenna for RFID reader in UHF band applications,” IEEE, 2015.

[20] Bijaya Shrestha, Atef Elsherbeni, and Leena Ukkonen, “UHF RFID Reader Antenna for Near-Field and Far-Field Operations,” IEEE Aantennas and Wireless Propagation Letters, Vol. 10, 2011.

[21] Chow-Yen-Desmond Sim, and Chin-Jen Chi, “A Slot Loaded Circularly Polarized Patch Antenna for UHF RFID Reader,” IEEE Antennas Propag, Vol. 60, No. 10, 2012.

[22] Hsin-lung Su, Sung-Lin Chen, “Design of a Circularly Polarized Antenna with Parasitic Square-Ring Strip for UHF RFID Reader Applications,” IEEE, 2015.

[23] T.A. Elwi, M.M. Hamed, Z. Abbas, and M.A. Elwi, “On the Performance of the 2D Planar Metamaterial Structure,” International Journal of Electronics and Communications, volume 68, issue 9, pp. 846–850, September 2014.

[24] T.A. Elwi, H.M. Al-Rizzo, D.G. Rucker, F. Song, “Numerical simulation of a UC–PBG lens for gain enhancement of microstrip antennas,” International Journal of RF and Microwave Computer-Aided Engineering, volume 19, issue 6, pp. 676–684, November 2009.

Author(s) biography

Ali Sadeq Abdulhadi Jalal was born in 1958 in Baghdad, Iraq. He earned the bachelor and master degrees in Electrical and Communication Engineering from the University of Technology, Baghdad, Iraq in 1980 and 1986 respectively. He finished his PhD at University Putra Malaysia (UPM) in 2013. His main research interests are in Antennas, Microwave devices, Analog and Digital Electronics.